

# Central Catadioptric Camera Calibration using Planar Objects<sup>\*</sup>

Cheng-I Chen<sup>1</sup> and Yong-Sheng Chen<sup>1\*\*</sup>

Department of Computer Science, National Chiao Tung University, Hsinchu, Taiwan

**Abstract.** Central catadioptric cameras combine lenses with mirrors to enlarge the field of view while keeping a single effective viewpoint. In this paper we propose a novel method of calibrating the intrinsic parameters of central catadioptric cameras using a planar object. Based on the viewing sphere model, we can warp a portion of the catadioptric image to an image captured by a virtual perspective camera with given intrinsic and extrinsic parameters. We show that placing the planar object several times around the catadioptric camera is equivalent to placing the same object at different poses relative to a static virtual perspective camera. Therefore, homography method can be applied to calculate the relative poses of the planar object as well as the projection error of feature points on the planar object. By minimizing the projection error, we can obtain the optimized intrinsic parameters of the central catadioptric camera. Besides simplicity, experiments with simulation and real image data clearly demonstrate the high robustness and accuracy of the proposed calibration method.

## 1 Introduction

Large field of view is important to the computer vision systems of video surveillance and robot navigation. There are many methods that can achieve this goal, including by rotating the imaging device, using fisheye lenses, and using catadioptric cameras [1]. Among these methods, catadioptric cameras combine reflective mirrors and refractive lenses to broaden the field of view [2–6]. They can be classified into two categories, central and non-central catadioptric cameras, depending on whether they preserve the single viewpoint constraint [7]. In this work we consider the central catadioptric cameras.

In the literature there are three major kinds of methods for calibrating the intrinsic parameters of central catadioptric cameras. Photogrammetric methods, the first kind, use calibration objects containing feature points with known 3-D coordinates [8]. Both extrinsic and intrinsic parameters can be obtained, at the expense of the costly construction of 3-D calibration objects. The second kind of calibration methods, self-calibration methods [9, 10], utilize corresponding

---

<sup>\*</sup> This work was supported in part by the Ministry of Economic Affairs, Taiwan, under Grant 95-EC-17-A-02-S1-032.

<sup>\*\*</sup> Corresponding author.



points in multiple views, instead of calibration objects. Although flexible, self-calibration is not robust because it is generally not easy to obtain accurate correspondence estimation. Due to the single viewpoint constraint, some properties of perspective geometry can also be applied to central catadioptric cameras. The third kind of calibration methods utilize geometric invariants without needing to know any metric information. For example, Geyer and Daniilidis [11] utilized the geometric invariants of space lines to calibrate the intrinsic parameters of para-catadioptric cameras. They also proposed a viewing sphere model for generalized central catadioptric cameras [12]. Based on this viewing sphere model, Barreto and Araújo [13] calibrated catadioptric camera by using three lines in space while Ying and Hu [14] did the calibration work by using three lines or two spheres in space.

In [15], Zhang proposed a flexible method of calibrating perspective cameras. This method has been widely used mainly due to its simplicity and accuracy. The calibration object is planar and can be easily produced by printing out a specially designed pattern. One simply places the planar object at a few orientations in front of the camera while capturing an image for each pose. Accurate camera parameters can then be obtained.

In this paper we propose a method of calibrating the central catadioptric cameras. The calibration procedure is as simple as that in [15]. We place a planar object several times around the catadioptric camera and capture a catadioptric image for each pose of the planar object. The planar object contains dense feature points and can cover the whole field of view of the catadioptric camera by combining the feature points on all the captured images. This good coverage will benefit the calibration accuracy. Based on the viewing sphere model, we warp the part of each catadioptric image containing the planar object to an image captured by a virtual perspective camera with given intrinsic parameters as well as extrinsic parameters relative to the viewing sphere. We show that placing the calibration object around the catadioptric camera is equivalent to placing the same object at different poses relative to a static virtual perspective camera. By utilizing the homography relationship, the set of warped images can be used to calculate the relative poses of the planar object as well as the reprojection error of feature points on the planar object. We can then optimize the intrinsic parameters of the central catadioptric camera, in a nonlinear fashion, by minimizing the reprojection error. Besides simplicity, experiments with simulation and real image data clearly demonstrate that the proposed calibration method is very robust and accurate.

## 2 Viewing Sphere Model for Central Catadioptric Camera

As shown by Baker and Nayar in [7], central catadioptric cameras can only be constructed by combining a perspective camera with a planar, ellipsoidal, or hyperboloidal mirror; or by combining an orthogonal camera with a parabolic mirror. In [12], Geyer and Daniilidis proposed a generalized image formation



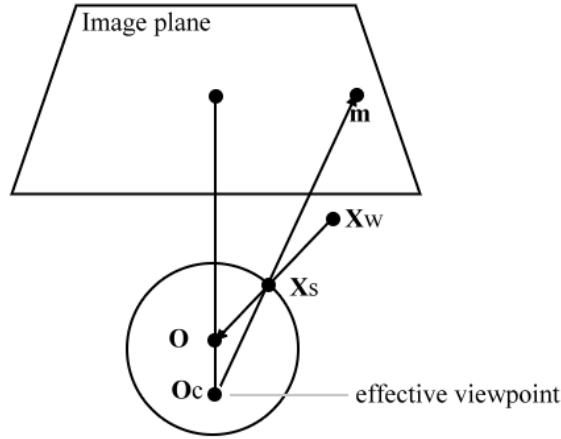


**Fig. 1.** Viewing sphere model for a catadioptric camera. The point  $\mathbf{X}_w$  is projected to the point  $\mathbf{X}_s$  on the surface of the viewing sphere, and then to the point  $\mathbf{m}$  on the image.

model, called the viewing sphere model, for catadioptric cameras. In this model, image formation of the central catadioptric camera can be described by a two-step mapping via the viewing sphere, which is a unit sphere centered at the origin  $\mathbf{O}$ , as shown in Fig. 1. First, the point  $\mathbf{X}_w = [x_w, y_w, z_w]^t$  is projected onto the viewing sphere surface at point  $\mathbf{X}_s = [x_s, y_s, z_s]^t$ , where

$$\mathbf{X}_s = \frac{\mathbf{X}_w}{\|\mathbf{X}_w\|} . \quad (1)$$

In the second step,  $\mathbf{X}_s$  is projected on the image plane at point  $\mathbf{m} = [m_x, m_y]^t$ , where the projection center is located at  $\mathbf{O}_c$ . The coordinate of point  $\mathbf{m}$  can be calculated by the following equation:

$$\lambda \begin{bmatrix} m_x \\ m_y \\ 1 \end{bmatrix} = \begin{bmatrix} r f_e & s & u_0 \\ 0 & f_e & v_0 \\ 0 & 0 & 1 \end{bmatrix} \begin{bmatrix} 1 & 0 & 0 & 0 \\ 0 & 1 & 0 & 0 \\ 0 & 0 & 1 & l \end{bmatrix} \begin{bmatrix} x_s \\ y_s \\ z_s \\ 1 \end{bmatrix} , \quad (2)$$

where  $\lambda$  is a scale factor and the intrinsic parameters of the catadioptric camera include the aspect ratio  $r$ , the effective focal length  $f_e$ , the skew factor  $s$ , the principal point  $[u_0, v_0]^t$ , and the distance between origin and the projection center  $l = \|\mathbf{O}\mathbf{O}_c\|$ . For the conic-section mirror,  $l$  can be computed as  $l = \frac{2\varepsilon}{1+\varepsilon^2}$ , where  $\varepsilon$  is the eccentricity of the conic section. The relationship between the eccentricity  $\varepsilon$  and the distance  $l$  for different central catadioptric cameras is shown in Table 1.



**Table 1.** Relationship between eccentricity  $\varepsilon$  and distance  $l$  in the viewing sphere model.

	Ellipsoidal	Paraboloidal	Hyperboloidal	Planar
$\varepsilon$	$0 < \varepsilon < 1$	$\varepsilon = 1$	$\varepsilon > 1$	$\varepsilon \rightarrow \infty$
$l$	$0 < l < 1$	$l = 1$	$0 < l < 1$	$l = 0$

From (2) we can easily calculate the forward projection between 3-D point and 2-D image point by

$$\begin{cases} m_x = \frac{r f_e x_s + s y_s + u_0 z_s + u_0 l}{z_s + l} \\ m_y = \frac{f_e y_s + v_0 z_s + v_0 l}{z_s + l} \end{cases}, \quad (3)$$

as well as the back projection by

$$\begin{cases} x_s = \frac{\lambda(f_e(m_x - u_0) - s(m_y - v_0))}{r f_e^2} \\ y_s = \frac{\lambda(m_y - v_0)}{f_e} \\ z_s = \lambda - l \\ x_s^2 + y_s^2 + z_s^2 = 1 \text{ (viewing sphere constraint)} \end{cases}. \quad (4)$$

### 3 Proposed Calibration Method

In this section we present the proposed calibration procedure. At first, we estimate the initial parameters of the viewing sphere model by using Ying's method [16]. We assume that the hyperboloidal mirror and the perspective camera of the central catadioptric system are aligned perfectly. The aspect ratio  $r$ , the skew factor  $s$ , and the principal point  $[u_0, v_0]^t$  of the viewing sphere model can be determined by calibration the perspective camera. The translation  $l$  can be calculated from the eccentricity of the hyperboloidal mirror,  $\varepsilon$ , as  $l = \frac{2\varepsilon}{1+\varepsilon^2}$ , while the effective focal length,  $f_e$ , of the viewing sphere model can be calculated as  $f_e = -\frac{1-\varepsilon^2}{1+\varepsilon^2}f$ , where  $f$  is the focal length of the perspective camera.

With the parameters of the viewing sphere model, we can dewarp a region of catadioptric image into a perspective image of a virtual perspective camera with specified intrinsic parameters. First, we select a point of interest  $\mathbf{m}_0$  in the catadioptric image, which is roughly at the center of the calibration object in our calibration procedure described later. Then we calculate its corresponding point on the unit sphere  $\mathbf{m}_s$  by using the backward projection equation (4) and determine a proper pose (that is, extrinsic parameters) relative to the viewing sphere so that the calibration object can be well captured by the virtual perspective camera. Once we have both the intrinsic and extrinsic parameters of the virtual camera, we can dewarp the catadioptric image onto the virtual perspective image plane, as shown in Fig. 2.

Of course the initial values of the parameters of the viewing sphere model may have deviation mainly from imperfection of the mirror, misalignment of the



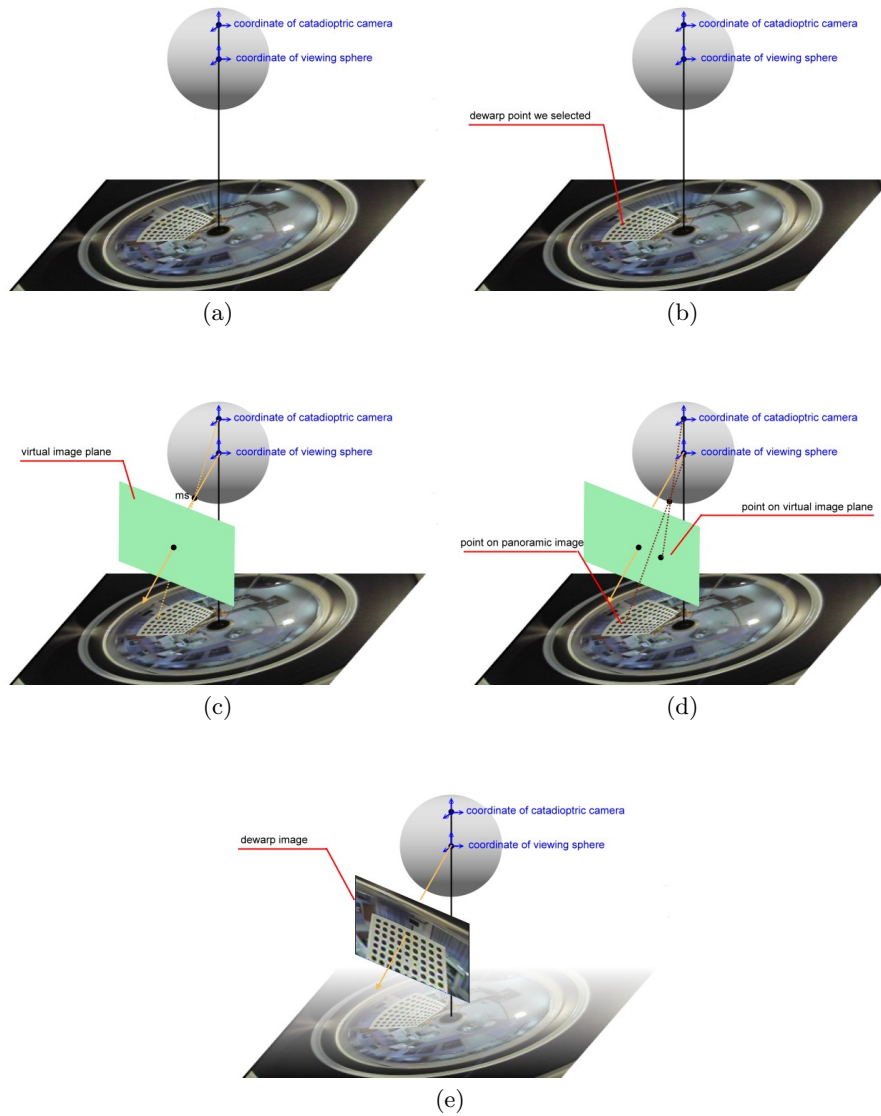


**Fig. 2.** From (a) to (e): Procedure of dewarping the catadioptric image onto a perspective image of a virtual camera.

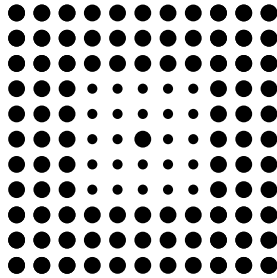


**Fig. 3. The calibration pattern used in this work. There are  $11 \times 11$  circles and the centroid of the central one is chosen as the origin.**

mirror, and inaccuracy of the eccentricity of the mirror (usually only nominal value is available). Therefore, it is a must to refine these parameters. If these parameters are ideally accurate, the dewarped image should be distortion-free perspective image. Otherwise, the dewarped image will be distorted and thus will increase the error of both forward and backward projection. In the proposed optimization procedure, we refine the intrinsic parameters of the central catadioptric cameras by minimizing the reprojection error of the feature points on a planar plate shown in Fig. 3. The calibration pattern contains  $11 \times 11$  grid-aligned circles with known relative positions, among them 24 circles around the central circle are smaller. This design facilitates easy identification of each circle and it is easy to locate the 2-D feature point in virtual perspective image by image binarization, blob analysis, and centroid estimation for each circle.

In the optimization procedure, we calculate virtual perspective image of the calibration pattern first. To calculate the calibration error, we need to estimate the relative pose between the constructed virtual perspective image and the planar plate. As aforementioned, the central catadioptric camera has a single projection center, and so does its constructed virtual perspective image. Therefore, we can estimate the relative pose between the planar pattern and the image plane by using conventional pose estimation method [15], with estimated feature points and their corresponding feature points on the planar pattern.

To achieve high calibration accuracy, the estimated feature points should cover all over the whole catadioptric image. Therefore, we need to place the calibration plate all around the catadioptric camera and capture enough images for proper coverage. We can dewarp each captured image to a perspective image, with respect to a virtual perspective camera as described previously. The intrinsic parameters and the projection center of the virtual cameras remain unchanged when dewarping all the captured catadioptric images. In this case we can see that moving a calibration plate around the catadioptric camera is equivalent to placing the same calibration plate at different poses relative to a static perspective camera, as shown in Fig. 4.

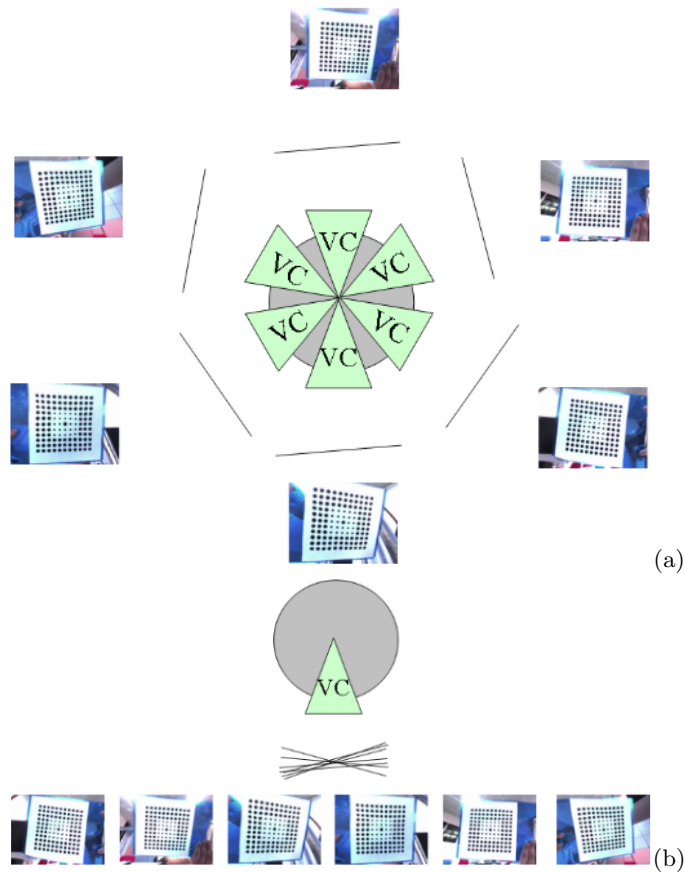


**Fig. 4.** (a) Moving a calibration plate around the catadioptric camera is equivalent to (b) placing the same calibration plate at different poses relative to a static perspective camera.

## 4 Experiments

### 4.1 Simulations

In this simulation, an ideal central catadioptric camera has been constructed with parameters  $f_e = 330$ ,  $s = 0$ ,  $r = 1$ ,  $l = 0.95$ ,  $u_0 = 512$  and  $v_0 = 384$ . The resolution of the image is  $1024 \times 768$ . The previously mentioned calibration pattern containing  $11 \times 11$  feature points were placed at seven positions around the catadioptric camera. Gaussian noise with zero-mean and  $\sigma$  standard deviation was added to these feature points in the image. We varied the noise level  $\sigma$  from 0.0 to 2.0 pixels and we perform 100 independent trials for each noise level.

The calibration results of the proposed method are shown in Table 2. In this table, the skew factor  $s$  is replaced by  $\theta$  which is the angle between the two image

**Table 2.** Calibration accuracy of simulation data using the proposed method.

$\sigma$	$f_e$ (%)	$\theta$ (%)	$r$ (%)	$l$ (%)	$u_0$ (%)	$v_0$ (%)	reprojection error
0	0.005	0.000	0.000	0.000	0.000	0.000	0.003
0.4	0.088	0.000	0.002	0.004	0.042	0.027	0.684
0.8	0.330	0.000	0.028	0.052	0.005	0.010	0.967
1.2	0.645	0.004	0.043	0.114	0.153	0.075	1.189
1.6	1.053	0.059	0.021	0.181	0.305	0.270	1.341
2.0	1.351	0.022	0.006	0.195	0.515	0.330	1.520

**Table 3.** Calibration accuracy of the proposed method with proper initial parameters.

	$(u_0, v_0)$	$r$	$s$	$f_e$	$l$	reprojection error
Initial	(547,393)	0.997	0.000	330.834	0.995	1.277
Optimized	(530,393)	1.008	-0.003	328.041	0.999	0.887

coordinate axes. The relative error of the effective focal length is calculated by  $(f_e - f_e^*)/f_e$ , where  $f_e$  is the ground truth and  $f_e^*$  is the mean of the estimated values. Relative error of other parameters are defined in the same way. The results show that the recovered parameters are accurate because the relative errors for each parameter is very small. When we increase the noise level, we can also obtain accurate camera parameters. Hence, these results demonstrate that our calibration method is accurate and robust.

## 4.2 Real Image Data

We also calibrated a central catadioptric camera combined by a perspective camera (Marlin F-080C) with a 16mm lens and a hyperbolic mirror. One of the captured image is shown in Fig. 5. The surface of the hyperboloidal mirror we used is described by  $\frac{x^2+y^2}{a^2} + \frac{z^2}{b^2} = -1$ , where  $a = 67.08$  and  $b = 150.0$ . The eccentricity of the hyperboloid is then  $\sqrt{1 + \frac{b^2}{a^2}} = 1.095439$ . The intrinsic parameters of the perspective camera are estimated by using Zhang's method [15]. According to these parameters, the initial parameters of viewing sphere model can be estimated, as shown in Table 3. The average reprojection error by using these initial parameters is calculated to be 1.277 pixels, as shown in Table 3. After the optimization procedure, the average reprojection error is reduced to 0.887 pixels.

For evaluating the performance of proposed optimization procedure, we specify a bad initial parameters of the viewing sphere model and verify whether the optimization procedure can recover. The virtual perspective images constructed by the initial parameters and optimized parameters are shown in Fig. 6. Obviously the virtual perspective image constructed by the initial parameters is seriously distorted. After the optimization procedure, the virtual perspective



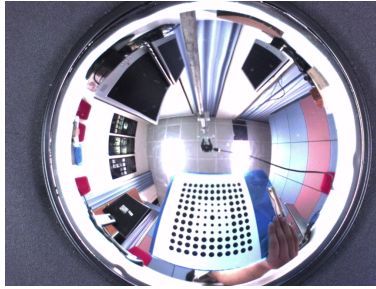


**Fig. 5.** Image captured by the central catadioptric camera constructed in this work.

**Table 4.** Calibration accuracy of the proposed calibration method with a bad initial parameters.

	$(u_0, v_0)$	$r$	$s$	$f_e$	$l$	reprojection error
Initial	(547,393)	1.000	0.000	530.000	0.800	4.729
Optimized	(547,393)	1.006	-0.005	368.196	0.994	1.197

image constructed by the refined parameters is much close to distortion-free perspective image. The calibration result is shown in Table 4. The average reprojection error of initial parameters is calculated to be 4.729 pixels. After the optimization procedure, the average reprojection error is reduced to 1.197 pixels.

## 5 Conclusions

In this work, we propose a novel calibration method to estimate the intrinsic parameters of central catadioptric camera systems. The calibration object is planar and is very easy to produce. Moreover, the calibration procedure is very simple. We only need to place the planar object several times around the catadioptric camera and its intrinsic parameters can be accurately estimated.

## References

1. Nayar, S.K.: Catadioptric omnidirectional camera. In: Proceedings of the IEEE Conference on Computer Vision and Pattern Recognition, IEEE Computer Society (1997) 482–488
2. Yagi, Y., Kawato, S.: Panoramic scene analysis with conic projection. In: Proceedings of IEEE/RSJ International Conference on Intelligent Robots and Systems. (1990)
3. Hong, J., Tan, X., Pinette, B., Weiss, R., Riseman, E.M.: Image-based homing. IEEE Control Systems (February 1992) 38–45
4. Yamazawa, K., Yagi, Y., Yachida, M.: Omnidirectional imaging with hyperboloidal projection. In: Proceedings of IEEE/RSJ International Conference on Intelligent Robots and Systems. Volume 2. (1993) 1029–1034



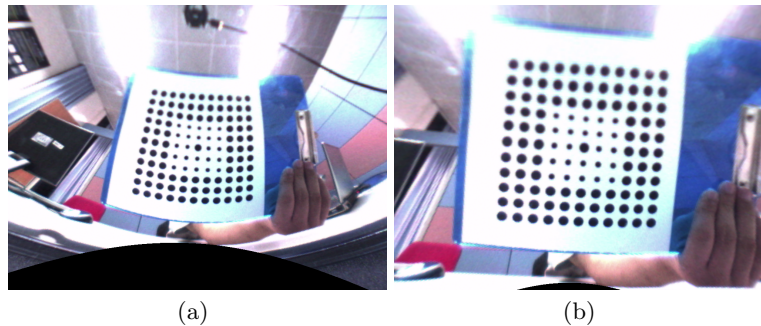


**Fig. 6.** Virtual perspective images constructed by (a) the initial guess and (b) the optimized parameters.

5. Nalwa, V.: A true omnidirectional viewer. Technical report, Bell Laboratories, Holmdel, NJ 07733, U.S.A. (1996)
6. Nayar, S.K., Baker, S.: Catadioptric image formation. In: Proceedings of Image Understanding Workshop. (1997) 1431–1438
7. Baker, S., Nayar, S.K.: A theory of catadioptric image formation. In: Proceedings of the IEEE International Conference on Computer Vision. (1998) 35–42
8. Aliaga, D.G.: Accurate catadioptric calibration for real-time pose estimation of room-size environments. In: Proceedings of the IEEE International Conference on Computer Vision. (2001) 127–134
9. Kang, S.: Catadioptric self-calibration. In: Proceedings of the IEEE Conference on Computer Vision and Pattern Recognition, Los Alamitos, IEEE (June 2000) 201–207
10. Mičušík, B., Pajdla, T.: Para-catadioptric camera auto-calibration from epipolar geometry. In: Proceedings of the Asian Conference on Computer Vision. Volume 2., Seoul, Korea South (January 2004) 748–753
11. Geyer, C., Daniilidis, K.: Catadioptric camera calibration. In: Proceedings of the IEEE International Conference on Computer Vision. (1999) 398–404
12. Geyer, C., Daniilidis, K.: A unifying theory for central panoramic systems and practical implications. In: Proceedings of the European Conference on Computer Vision. (2000) II: 445–461
13. Barreto, J.P., Araújo, H.: Geometric properties of central catadioptric line images and their application in calibration. *IEEE Transactions on Pattern Analysis and Machine Intelligence* **27**(8) (2005) 1327–1333
14. Ying, X., Hu, Z.: Catadioptric camera calibration using geometric invariants. *IEEE Transactions on Pattern Analysis and Machine Intelligence* **26**(10) (2004) 1260–1271
15. Zhang, Z.: A flexible new technique for camera calibration. *IEEE Transactions on Pattern Analysis and Machine Intelligence* **22**(11) (2000) 1330–1334
16. Ying, X., Hu, Z.: Can we consider central catadioptric cameras and fisheye cameras within a unified imaging model. In: Proceedings of the European Conference on Computer Vision. (2004) Vol I: 442–455